SPANDIDOS PUBLICATIONS

EXPERIMENTAL AND THERAPEUTIC MEDICINE 13: 851-860, 2017

Impact of gabapentin on neuronal high voltage-activated Ca^{2+} channel properties of injured-side axotomized and adjacent uninjured dorsal root ganglions in a rat model of spinal nerve ligation

MINMIN ZHU[1,2*], XIAODI SUN[3*], XIAODONG CHEN[3], HANG XIAO[4], MANLIN DUAN[1] and JIANGUO XU[1]

[1]Department of Anaesthesiology, Jinling Hospital, School of Medicine, Nanjing University, Nanjing, Jiangsu 210002;
[2]Department of Anaesthesiology, Wuxi Second Hospital, Nanjing Medical University, Wuxi, Jiangsu 214002;
[3]Department of Anaesthesiology, First Hospital, Nanjing Medical University, Nanjing, Jiangsu 210002;
[4]Department of Toxicology, School of Public Health, Nanjing Medical University, Nanjing, Jiangsu 210029, P.R. China

Received July 20, 2015; Accepted September 27, 2016

DOI: 10.3892/etm.2017.4071

Abstract. The density and properties of ion channels in the injured axon and dorsal root ganglion (DRG) neuronal soma membrane change following nerve injury, which may result in the development of neuropathic pain. Gabapentin (GBP) is a drug for the first-line treatment of neuropathic pain. One of its therapeutic targets is the voltage-activated calcium channel (VACC). In the present study, the whole-cell patch clamp technique was used to examine the changes of high voltage-activated Ca^{2+} (HVA-Ca^{2+}) channels in DRG neurons from sham and neuropathic rats in the absence and presence of GBP. The results demonstrated a reduction in peak current density and the 'window current' between activation and inactivation in adjacent and axotomized neurons from rats that had undergone L_5 spinal nerve ligation, thus attenuating the total inward Ca^{2+} current. Following the use of the specific channel blockers nifedipine, ω-conotoxin MVIIC and ω-conotoxin MVIIA, increased HVA-Ca^{2+} channels as well as an increased proportion of N-type Ca^{2+} currents were observed in axotomized neurons. GBP inhibited HVA calcium channel currents in a dose-dependent manner. The activation and steady-state inactivation curves for HVA channels were shifted in a hyperpolarizing direction by 100 μmol/l GBP. Following the application of GBP, a reduction in the 'window current' was observed in control and axotomized neurons, whereas the 'window current' was unchanged in adjacent neurons. This indicates that the inhibitory effects of GBP may be dependent on particular neuropathological or inflammatory conditions. The proportion of N-type Ca^{2+} currents and sensitivity to GBP were increased in axotomized neurons, which indicated the involvement of N-type Ca^{2+} currents in the inhibitory effect of GBP.

Correspondence to: Dr Jianguo Xu, Department of Anaesthesiology, Jinling Hospital, School of Medicine, Nanjing University, 305 East Zhongshan Road, Nanjing, Jiangsu 210002, P.R. China
E-mail: jianguoxucn@126.com

*Contributed equally

Key words: spinal nerve ligation, dorsal root ganglion, high-voltage-activated Ca^{2+} channel, gabapentin

Introduction

Neuropathic pain results from lesions to the peripheral nervous system (PNS) caused by infection, mechanical trauma, neurotoxic chemicals, metabolic diseases or tumor invasion (1). It involves a number of pathophysiological changes that occur within the central and peripheral nervous systems (1). Afferent discharge may emanate from the injury site and neuronal somata in the dorsal root ganglion (DRG), or even elsewhere along the injured axons in response to certain physical or chemical stimuli. This may lead to peripheral and central sensitization, an important causative factor for the onset and maintenance of neuropathic symptoms, including spontaneous pain, hyperalgesia and allodynia (1,2). Following peripheral nerve injury, the ipsilateral injured side contains injured and intact sensory axons and neurons.

L_5 spinal nerve ligation (SNL) is an experimental neuropathic pain model exhibiting a clear separation between injured and non-injured cell bodies (3). It has been demonstrated that almost all L_5 DRG neurons were axotomized following transection of the L_5 spinal nerve, while the L_4 ganglionic cells infiltrated the degenerating L_5 axonal environments. The contribution of injured and intact sensory neurons to the onset and maintenance of neuropathic pain is controversial (4). Sapunar *et al* (5) observed that distinct electrophysiological changes occur in injured and adjacent DRG membranes. The afterhyperpolarization (AHP) duration in L_5 neurons with C fibers shortened following axotomy, while adjacent L_4 neurons showed no change in action

potential duration, AHP dimensions or excitability following SNL. However, an *in vivo* study demonstrated that, following SNL, electrophysiological changes occurring in large- and medium-sized somata of intact (L_4) as well as axotomized (L_5) DRG neurons were similar and included a longer action potential (AP) duration, slower AP rise and falling rates, a lower current and voltage threshold, and a higher input resistance (6).

Following peripheral nerve lesion, the distribution and properties of transmembrane ion channels in injured axons and DRG neurons change, leading to alterations in the excitability and conductive properties of peripheral afferent fibers (7). DRG neurons express a variety of VACCs, a family of transmembrane proteins widely distributed in excitable cells and also detected in a number of non-excitable cells. When the plasma membrane becomes depolarized, the VACC channels open, mediating Ca^{2+} entry in response to sub-threshold depolarizing signals and APs (8). α2δ1 is the most abundant VACC sub-type in the spinal cord and DRG, and co-expression of α2δ1 with α1 and β VACC sub-units *in vitro* results in accelerated activation, inactivation kinetics and increased calcium current density (9). Increased α2δ1 sub-unit expression and calcium channel activity in the dorsal horn have been observed in neuropathic pain (10). Furthermore, it has been demonstrated that gabapentin (GBP), the first-line drug for the treatment of neuropathic pain, specifically binds to the α2δ1 sub-unit of N-type VDCCs and exerts various actions responsible for pain attenuation (11).

In the present study, nerve injury-induced changes in the electrophysiological properties of DRG high-voltage activated (HVA)-Ca^{2+} currents were examined, as well as the influence of GBP on these changes in injured-side axotomized and adjacent uninjured DRGs in model rats subjected to SNL.

Materials and methods

Surgical procedure. A total of 96 healthy male Sprague-Dawley (SD) rats (age, 4-6 weeks*;* weight, 120-150 g) were purchased from the Model Animal Research Center of Nanjing University (Nanjing, China). They were kept under a temperature of 22-24˚C, a humidity of 50-60% and a 12 h light-dark cycle. All rats had *ad libitum* access to food and water. Rats were randomly divided into two groups: An SNL group (n=60) and a sham group (n=36). The 60 rats in the SNL group received a unilateral, tight ligation and transection of the left L_5 spinal nerve using a modification of the surgical procedure previously described by Kim and Chung (12). In brief, under anesthesia with 2% pentobarbital sodium administered intraperitoneally (i.p., 50 mg/kg; Sigma-Aldrich; Merck Millipore, Darmstadt, Germany) and following exposure of the left L_5 spinal nerve, the left L_5 and L_4 spinal nerves were identified. The left L_5 spinal nerve was separated and tightly ligated with 5-0 silk sutures between the DRG and the conjunction to form the sciatic nerve and transected just distal to the ligature. The 36 sham rats underwent exposure, while they did not undergo ligation or transection of the spinal nerve. The present study was performed in strict accordance with the recommendations in the Guide for the Care and Use of Laboratory Animals of the National Institutes of Health. The experimental animal protocol was reviewed and approved by the Institutional Animal Care and Use Committee of Nanjing University (Nanjing, China).

Behavioral tests. All experimental rats were subjected to behavioral tests at 1 day prior to as well as 1, 3, 7 and 14 days following surgery. All tests were repeated three times.

To assess tactile allodynia, rats in clear plastic cages with a wire mesh bottom were tested using an up-down method as described by Choi *et al* (13). A filament (Supertips™ flexible Von Frey hairs, IITC Life Science, Woodland Hills, CA, USA) with a suitable, calibrated buckling weight was applied to the plantar surface of the hind paw with pressure causing the filament to bend. Absence of paw lifting after 4 sec led to the use of the next filament with increased weight, whereas paw lifting indicated a positive response and led to the use of the next weaker filament. This paradigm continued until the withdrawal threshold was estimated as the smallest fiber size that evoked at least three withdrawal responses during five consecutive applications with the same fiber.

A von Frey mechanical pain threshold detector (Model 2390 Electric von Frey aesthesiometer; IITC Life Science) was used to assess mechanical hyperalgesia. A paw-flick response was elicited by applying increasing force (in g) using rigid tips (400 g; Model 2391; IITC Life Science) focused on the plantar surface of the hindpaw. The force applied that elicited a reflex removal of the hindpaw was recorded.

Thermal hyperalgesia was determined by comparison of paw withdrawal latency to thermal stimuli between operated and non-operated sides. Rats were exposed to a radiant source generated and controlled by an IITC Model 390 Analgesia Meter (10 V; 30 W; spot dimensions, 4x6 mm; IITC Life Science). The light radiation intensity was set at 50% with intervals of 30 sec (in order to avoid extensive damage).

Dissociation of DRG neurons. At 15 days after surgery, rats in the SNL or sham group were anesthetized with 2% pentobarbital sodium (50 mg/kg i.p., Sigma-Aldrich; Merck Millipore) for the dissociation of DRG neurons. The L_4 and L_5 DRGs and attached dorsal roots were removed and the connective tissue capsule was dissected using microdissection scissors in ice-cold, oxygenated, buffered Dulbecco's modified Eagle's medium (DMEM, High Glucose, Gibco; Thermo Fisher Scientific, Inc., Waltham, MA, USA) containing 3.7 g/l $NaHCO_3$ (pH 7.2). DRG fragments were rinsed with DMEM three times and subsequently transferred into 1.5 ml DMEM containing 2 mg/ml type I collagenase (Sigma-Aldrich; Merck Millipore) and 1.2 mg/ml type I trypsin (Sigma-Aldrich; Merck Millipore) and aerated with 5% CO_2 and 95% O_2 at 36.5˚C for 25 min until complete dissociation was confirmed microscopically. DRG neurons were rinsed in an oxygenated, standard extracellular solution containing 145 mmol/l tetraethylammonium chloride, 0.8 mmol/l $MgCl_2$, 5 mmol/l $CaCl_2$, 20 mmol/l 4-(2-hydroxyethyl)-1-piperazineethanesulfonic acid (HEPES; Sigma-Aldrich, Merck Millipore) and 10 mmol/l D-glucose (the pH was adjusted to 7.3 with Tris base) to terminate the enzyme reactions. Individual neurons were dissociated by passing DRG fragments through a set of fire-polished glass pipettes. Finally, neurons were plated onto culture dishes consisting of extracellular solution through the

coated metallic screen (250 mesh, WS Tyler, Mentor, OH, USA). Cells were allowed to attach to the culture dishes for 2-3 h at room temperature.

Whole-cell patch-clamp recording. Neurons were studied 8-10 h after dissociation. Cells were visualized with an inverted microscope and their soma diameter was determined as small (<30 μm), medium (30-40 μm) or large (>40 μm) with the aid of a calibrated microscope eyepiece reticle (Olympus Corporation, Tokyo, Japan). The subsequent analysis focused on the medium-diameter neurons, which were considered as the nociceptive afferent (Aδ and C fibres, slow-conducting velocities) and low-threshold sensory afferent (14).

Whole-cell configuration of the patch-clamp technique was used for current clamp and voltage-clamp electrophysiological recordings using the EPC-9 patch-clamp amplifier (HEKA Elektronik, Lambrecht, Germany) with an AgCl reference electrode. Electrical stimuli pulses and current recording were controlled and performed using PULSE+PULSEFIT ver. 8.79 (HEKA Elektronik). Channel currents were sampled using the ITC-16 data acquisition system (InstruTech; HEKA Elektronik). Recordings were acquired at 20 kHz, filtered at 2 kHz and sampled using a computer with Digidata 1200 A/D acquisition board (HEKA Elektronik) for offline analyses. Sigmaplot ver. 10.0 (Systat software, Inc., San Jose, CA, USA) was used for data analysis. The current-voltage curves were generated using Igor pro 4.0 (WaveMetrics, Inc., Lake Oswego, OR, USA) software.

Micro-electrodes were pulled from glass capillaries (diameter, 1.6 mm; Beijing Xianqu Weifeng Technology Development Co., Beijing, China) using a pipette puller (PP-830; Narishige Scientific Instrument Lab., Tokyo, Japan). The diameter of the micro-electrode tip was 1-2 mm. The resistance of the internal solution [CsCl 135 mmol/l, $MgCl_2$ 2 mmol/l, EGTA 11 mmol/l, $CaCl_2$ 1 mmol/l, HEPES 20 mmol/l, magnesium-adenosine triphosphate (Mg-ATP) 5 mmol/l, guanosine 5'-triphosphate lithium salt (Li-GTP) 0.4 mmol/l, pH 7.3], filled into pipettes was 3-6 MΩ. Micropipettes were positioned on the membrane and gentle suction was applied to obtain a resistant seal in the GΩ range (>1 GΩ). Following rupture of the membrane with suction at negative pressure, entering the whole-cell recording configuration, neurons were allowed to reach adequate equilibration between the internal pipette solution and the cell interior for 10 min. The slow capacitance, system resistance, series resistance, capacitance current and leakage current were electronically compensated with the compensation circuitry of the amplifier during current recording. Effective data was defined as a steady current and series resistance <20 MΩ.

Drug application. Drugs were added to extracellular solution, bathing the dissociated DRG neurons. Fluid changes and continuous perfusions were achieved through a gravity-dependent flow system. Stocks of GBP, ω-conotoxin MVIIC, ω-conotoxin MVIIA, $CdCl_2$ and Li-GTP (Sigma-Aldrich; Merck Millipore) were prepared in distilled water and stored at -20˚C.

Data analysis and statistics. The current density of certain cells was obtained from the inward current standardized by the membrane capacitance and compared with those of other cells. The voltage-dependent current curve was fit according to the Boltzmann equation, $G/G_{max}=1/\{1+\exp[(Va_{1/2}-Vm)/Ka]\}$, where G is the conductance calculated as $G=I/(V_m-V_r)$, where I is the current, V_m is the command voltage, V_r is the reversal potential, $Va_{1/2}$ is the voltage at the half maximal activation current and Ka is the slope factor describing the voltage dependence of the conductance. The curve of the steady-state inactivation current was fit according to the Boltzmann equation, $I/I_{max} = 1 / \{1 + \exp [(V - Vi_{1/2}) / Ki]\}$, where I is the current, V is the pre-stimulus voltage, $Vi_{1/2}$ is the voltage at the half maximal inactivation current and *K*i is the slope factor of inactivation.

SPSS statistical software ver. 16.0 (SPSS Inc., Chicago, IL, USA) was used for statistical analysis. Values are expressed as the mean ± standard deviation. Two-way analysis of variance was used for comparison among groups and the q test was used for pairwise comparison. Statistical analysis between any two groups was performed using the group *t*-test and a paired *t*-test was used for comparison of pre- and post-drug application within groups. P<0.05 was considered to indicate a statistically significant difference.

Results

Confirmation of establishment of the rat model of neuropathic pain. All SNL-treated rats that underwent electrophysiological analysis exhibited clear behavioral indications of allodynia, mechanical hyperalgesia and thermal hyperalgesia. Prior to surgery, no significant differences in the mean foot withdrawal threshold were observed between the contralateral and ipsilateral feet of the mice in each group as well as between the SNL and sham groups. Mean withdrawal thresholds obtained from the feet ipsilateral to the SNL decreased significantly on the first post-operative day and remained significantly lower than the pre-operative value for up to 14 post-operative days (P<0.05; Fig. 1A and B). By contrast, there were no significant changes in the withdrawal threshold in paws contralateral to the SNL between the groups or for either foot in the sham-operated group. The latency for foot withdrawal in SNL rats significantly decreased in response to thermal stimuli delivered to the ipsilateral foot on the first post-operative day and remained lower during the entire observation period, compared with the non-operated side in the SNL rats (P<0.05; Fig. 1C). However, latency was not affected by the sham operation.

Dose-dependent inhibition of the HVA-Ca^{2+} peak current by GBP. After entering the whole-cell recording configuration, inward currents were activated under the command voltage from -70 to +40 mV at 80-msec intervals in 10 mV increments and with a holding potential (V_H) of -90 mV. There were no low-voltage-activated (LVA) components and no fast component of inactivation in the inward currents. Activation of inward currents occurred at -40 mV and peak inward currents occurred at 0 mV according to the current density-potential (I-V) curve. Inward currents were completely suppressed following the addition of 200 μmol/l $CdCl_2$ with the same stimuli, which was in accordance with the properties of HVA-Ca^{2+} currents (Fig. 2).

Voltage steps of 80 msec were applied to various test potentials between -70 and +40 mV in 10-mV steps with

Table I. Comparison of peak current inhibition rates (%) among the three groups at various gabapentin concentrations.

	Gabapentin concentration (μmol/l)				
Group	0.1	1	10	100	300
C (n=7)	10.8±1.5	12.8±1.8	15.6±2.1[a]	27.3±2.9[a,b]	28.1±3.3[a,b]
SNL-L_4 (n=5)	10.5±1.6	12.2±2.1	16.0±1.9[a]	26.9±2.0[a,b]	27.4±2.3[a,b]
SNL-L_5 (n=8)	11.4±1.5	12.9±1.0	18.5±1.7[a,c,d]	32.0±2.6[a-d]	32.7±2.8[a-d]

Values are expressed as the mean ± standard deviation (n=8). [a]P<0.05, intragroup comparison between 0.1 and 1 μmol/l; [b]P<0.05, compared with 10 μmol/l of the same group; [c]P<0.05, compared with the C group of the same concentration; [d]P<0.05, compared with the SNL-L4 group at the same concentration. SNL, spinal nerve ligation; L4, adjacent neurons; L5, axotomized neurons; C, control.

5-sec intervals from a V_H of -90 mV. This was performed to examine current-voltage associations in axotomized, adjacent neurons and control neurons from the L_4 and L_5 DRGs and attached dorsal roots of sham-operated rats. Peak inward calcium current levels were measured, corrected for cell size and subsequently expressed as the peak current density (pA/pF). Peak current densities of control, adjacent and axotomized neurons were 144±24, 104±17 and 75±17 pA/pF, respectively. Compared with that of control neurons, the peak current density of adjacent and axotomized neurons decreased significantly (P<0.05) and the peak current density of axotomized neurons was significantly lower than that of adjacent neurons (P<0.05). The activation voltage of the peak HVA-Ca^{2+} current density in control and adjacent neurons was 0 mV, while that of axotomized neurons was -10 mV (Fig. 3).

Steady maximal activation of HVA-Ca^{2+} currents was achieved with a voltage of V= 10 or 0 mV at 80-msec intervals and the dose-dependent inhibition effect of GBP was subsequently determined using 0.1, 1, 10, 100 and 300 μmol/l GBP. Changes in peak inward Ca^{2+} flux (ICa) were recorded and the inhibition of currents with GBP at various doses was calculated. The peak ICa was significantly enhanced in cells exposed to higher concentrations of GBP (10, 100 and 300 μmol/l; P<0.05), in comparison with cells exposed to lower concentrations of GBP (0.1 and 1 μmol/l). GBP significantly inhibited the peak inward ICa in a dose-dependent manner. Furthermore, the inhibitory effects of GBP on the peak current of axotomized neurons at concentrations of 10, 100 and 300 μmol/l were significantly higher than those on the current of control and adjacent neurons (P<0.05). There were no significant differences in the inhibitory effects on the peak current between control and adjacent neurons at various concentrations of GBP (P>0.05; Table I).

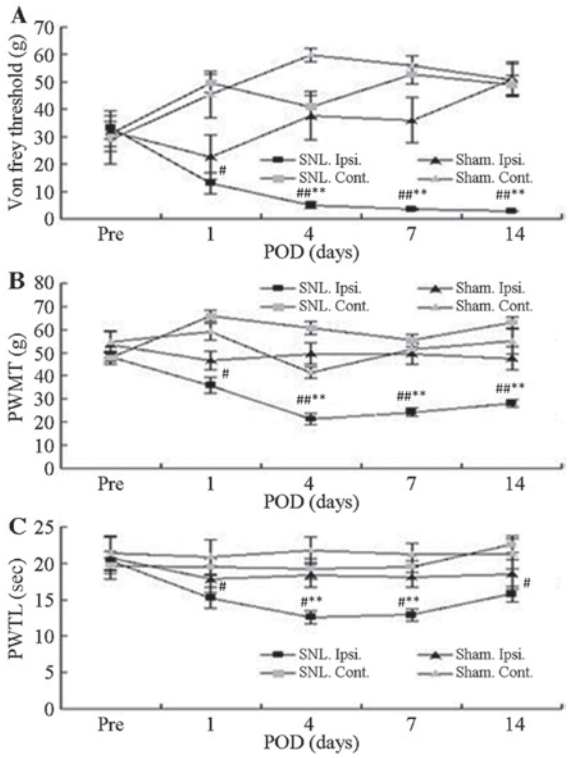

Figure 1. Withdrawal responses of Ipsi. and Cont. feet following mechanical and thermal stimulation. (A) Mean threshold for withdrawal following Von Frey stimulation with different bending forces. (B) Thresholds of paw withdrawal in response to mechanical stimuli. (C) Mean latencies of thermal withdrawal responses. Values are expressed as the mean ± standard deviation. #P<0.05 and ##P<0.01, Pre vs. Pod (paired *t*-test); *P<0.05 and **P<0.01, Ipsi. foot responses in SNL (n=16) vs. sham group (n=7) (analysis of variance). Pre, pre-operative period; Pod, post-operative days; Ipsi., paw ipsilateral to surgery; Cont., paw contralateral to surgery; PWMT, paw withdrawal mechanical threshold; PAWTL, paw withdrawal time latency; SNL, spinal nerve ligation; sham, sham operation.

Effects of GBP on the kinetics of HVA-Ca^{2+} channels. The membrane V_H was set at -90 mV and calcium currents were elicited by a series of command voltages (range, -70 to +40 mV) with successive increments of 10 mV at 80-msec intervals. As shown in Fig. 4, the midpoint potentials for the activation curves ($Va_{1/2}$) of control, adjacent and axotomized neurons were -16.23±1.92, -18.03±0.37 and -20.73±0.33 mV, respectively, with the $Va_{1/2}$ of axotomized neurons being significantly lower than that of the control and adjacent neurons (P<0.05; Fig. 4C); however, no difference was observed between those of the control and adjacent neurons (P>0.05; Fig. 4C). To study the kinetics of channel inactivation, calcium currents were generated by applying a membrane V_H at -90 mV for 10 msec, followed by series of command voltages from -70 to +20 mV with successive increments of 10 mV at 500-msec intervals. Subsequently, command voltages of -10 mV at 80-msec intervals were applied. The midpoint potentials for the inactivation curves ($Vi_{1/2}$) of control, adjacent and axotomized neurons were

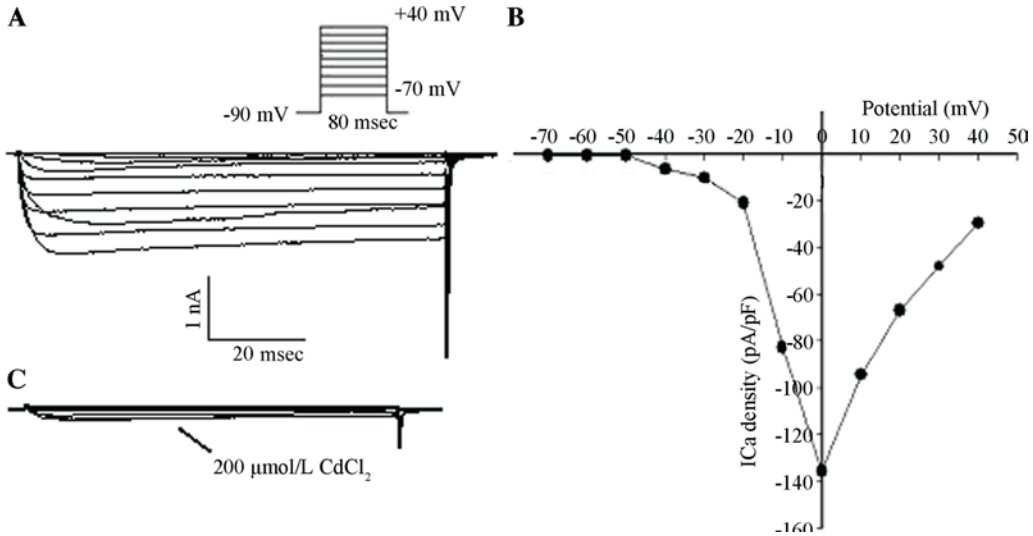

Figure 2. HVA calcium channel currents. (A) Inward currents were recorded with the command voltage between-70 and +40 mV with 80-msec intervals and successive increments of 10 mV, as well as a VH of -90 mV. (B) The I-V curve was fit using a Boltzmann equation. The ICa density was the Ca^{2+} channel current standardized by the membrane capacitance. (C) Inward currents in the same cell were recorded using the same steps of command voltages as in A in the presence of 200 μmol/l $CdCl_2$. HVA, high-voltage activation; ICa, Ca^{2+} currency; V_H, holding potential; I-V, current-voltage, pA/pF, peak current density.

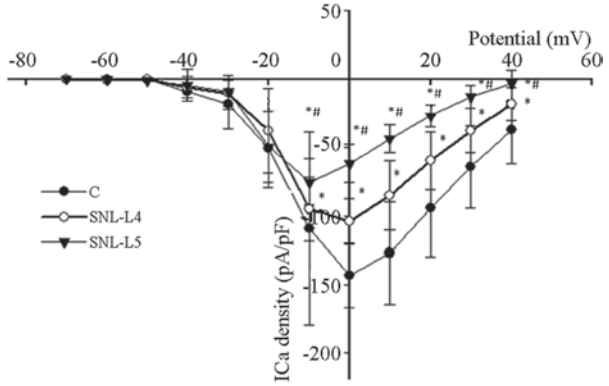

Figure 3. ICa density-voltage associations in control, adjacent and axotomized neurons were examined by the application of 80-msec voltage steps to various test potentials between -70 and +40 mV in 10-mV steps with 5-sec intervals from a holding potential of -90 mV. The ICa of adjacent (104±17 pA/pF; n=5) and axotomized neurons (75±17 pA/pF; n=8) was significantly lower than that of control neurons (144±24 pA/pF; n=7; P<0.05). In addition, the ICa of axotomized neurons was lower than that of adjacent neurons (P<0.05). The activation voltage of ICa in control and adjacent neurons was 0 mV, while that in axotomized neurons was -10 mV. Values are expressed as the mean ± standard deviation. *P<0.05 vs. control neurons. #P<0.05 regarding adjacent vs. axotomized neurons. ICa, Ca^{2+} density; pA/pF, peak current density; C, control; SNL, spinal nerve ligation; L4, adjacent neurons; L5, axotomized neurons.

-31.93±1.03, -31.45±1.87 and -32.73±1.37 mV, respectively. There were no significant differences in the midpoint potentials among the three types of neurons (P>0.05; Fig. 4D).

To study the effects of GBP on the kinetics of HVA-Ca^{2+} channel activation, I-V associations for the transient calcium channel currents were plotted using 10-mV incremental step pulses from -70 to +40 mV at 80-msec intervals with a membrane V_H at -90 mV in the presence of 100 μmol/l GBP. The $Va_{1/2}$ decreased from -16.23±1.92 to -19.69±1.07 mV (P<0.05), -18.03±0.37 to -21.73±0.64 mV (P<0.05) and -20.73±0.33 to -23.94±0.15 mV (P<0.05) in the control, adjacent and axotomized neurons, respectively (Fig. 5). To investigate the effects of GBP on the kinetics of HVA-Ca^{2+} channel inactivation, steady-state inactivation was measured in a conventional way using a 500-msec pre-pulse from -70 to +20 mV in 10-mV increments with a -90-mV membrane V_H for 10 msec followed by a second test pulse at -10 mV for 80 msec in the presence of 100 μmol/l GBP. By addition of 100 μmol/l GBP, the current required to inactivate Va1/2 was decreased from -38.78±2.05 to -31.93±1.03 mV in control neurons, from -36.22±2.80 to -31.45±1.87) mV in adjacent neurons and from -44.23±2.30 to -32.73±1.37 mV in axotomized neurons (Fig. 5).

The voltage dependence of activation shifted in a depolarized direction, whereas the $Vi_{1/2}$ remained unchanged in axotomized as well as adjacent uninjured DRG neurons, compared with those in control neurons. The shift in activation reduced the 'window current' between inactivation and activation, thereby stopping the sustained inward ICa. Following the addition of GBP, the activation and steady-state $Vi_{1/2}$ of three groups all shifted in a hyperpolarized direction. The shift in activation and inactivation reduced the overlap ('window currents') between inactivation and activation in control and axotomized neurons, while the 'window currents' remained unchanged in adjacent neurons (Fig. 5).

Effects of SNL injury and GBP on HVA-Ca^{2+} channel currents. Maximal activation of the HVA-Ca^{2+} currents occurred with V=10 or 0 mV at 80-msec intervals, with a membrane V_H of -90 mV. To individually assess different sub-types of HVA-Ca^{2+} channels present in the same cell, 20 μmol/l nifedipine (L-type calcium channel blocker), 2 μmol/l ω-conotoxin MVIIC (P/Q-type calcium channel blocker) and 2 μmol/l ω-conotoxin MVIIA (N-type calcium channel blocker) were applied to the bath in sequence when stable currents were reached. Similar activation voltages were applied to the same cells to evoke Ca^{2+} currents. Currents subtracted prior to and following application of respective blocker yielded L-, N-, P/Q-type currents. Subsequently,

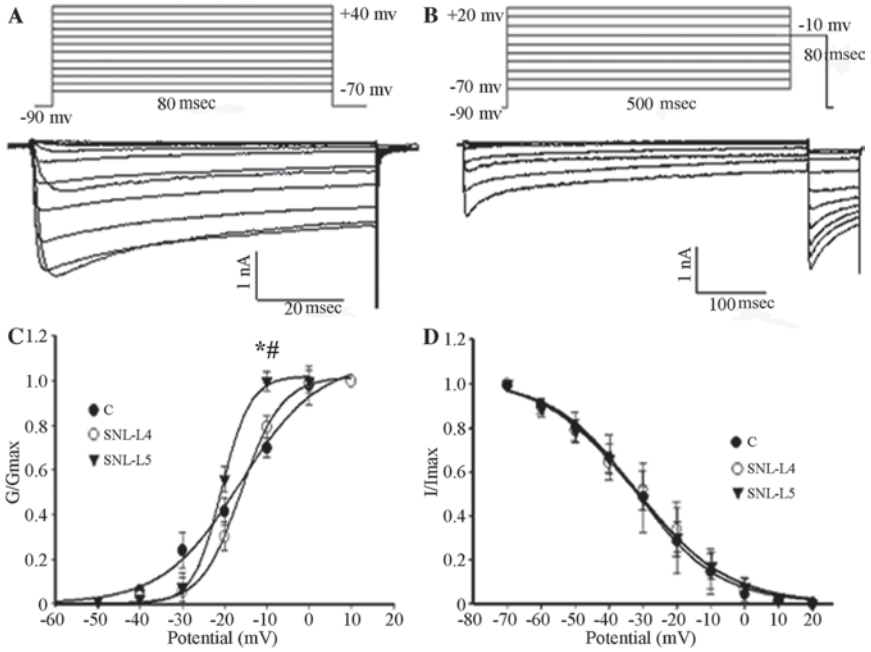

Figure 4. (A) Activation. The membrane V_H was set at -90 mV, calcium currents were elicited by a series of command voltages ranging from -70 to +40 mV with successive increments of 10 mV with 80-msec intervals. (B) Steady-state inactivation. Ca^{2+} currents were generated by the membrane VH at -90 mV for 10 msec, immediately followed by a series of command voltages from -70 to +20 mV with successive increments of 10 mV at 500-msec intervals. Subsequently, command voltages of -10 mV were applied at 80-msec intervals. (C) Activation curves were fitted using the Boltzmann equation (control neurons, n=10; adjacent neurons, n=5; axotomized neurons, n=8). A depolarized shift was observed in adjacent and axotomized neurons. Va1/2 of three groups was compared. *P<0.05 vs. control neurons. #P<0.05 regarding axotomized vs. adjacent neurons. (D) Inactivation curves were fitted using the Boltzmann equation (control neurons; n=6; adjacent neurons, n=6; axotomized neurons, n=7). Vi1/2 of three groups was compared. Values are expressed as the mean ± standard deviation. C, control; SNL, spinal nerve ligation; V_H, holding potential; G, conductance; I, current; L4, adjacent neurons; L5, axotomized neurons.

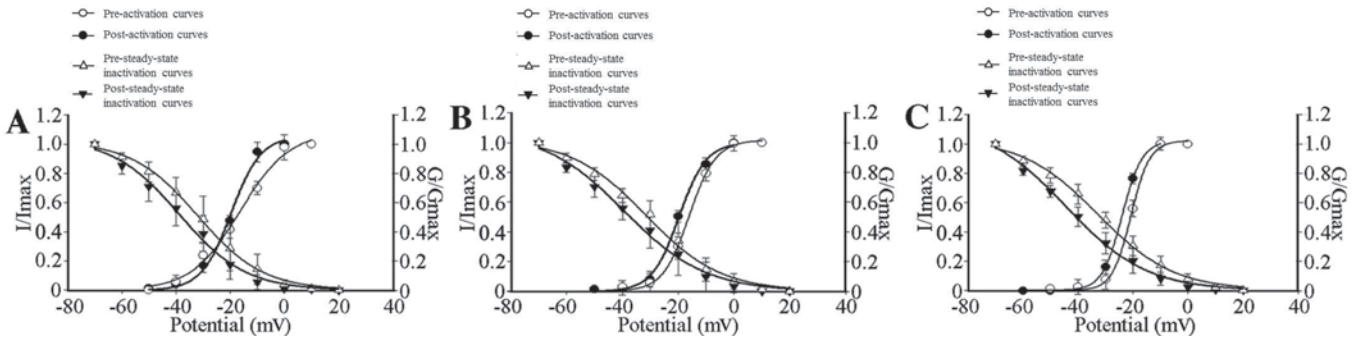

Figure 5. HVA-Ca^{2+} current activation and steady-state inactivation curves of control, adjacent and axotomized neurons in the absence or presence of 100 μmol/l GBP. (A) Activation (n=10) and steady-state inactivation (n=6) curves shifted towards a hyperpolarization direction in control neurons, which reduced the 'window currents', in the presence of 100 μmol/l GBP. $Va_{1/2}$ decreased from -16.23±1.92 to -19.69±1.07 mV with GBP added (P<0.05); $Vi_{1/2}$ was inactivated at -31.93±1.03 mV vs. -38.78±2.05 (P<0.05). (B) A hyperpolarized shift was observed in activation (n=5) and steady-state inactivation (n=6) curves of adjacent neurons; however, 'window currents' remained unchanged in the presence of 100 μmol/l GBP. $Va_{1/2}$ decreased from -18.03±0.37 to -21.73±0.64 mV (P<0.05) with the addition of GBP; $Vi_{1/2}$ was inactivated at -31.45±1.87 mV vs. -36.22±2.80 mV (P<0.05). (C) Activation (n=8) and steady-state inactivation (n=7) curves in axotomized neurons, showing reduced 'window currents' in the presence of 100 μmol/l GBP. Compared without using GBP, after adding GBP, $Va_{1/2}$ and $Vi_{1/2}$ decreased from -20.73±0.33 and -32.73±1.37 mV towards -23.94±0.15 mV (P<0.05) and -44.23±2.30 mV (P<0.05). Values are expressed as the mean ± standard deviation. GBP, gabapentin; HVA, high-voltage activation; $Va_{1/2}$, voltage at the half maximal activation current; $Vi_{1/2}$, voltage at the half maximal inactivation current; I, current; G, conductance.

100 μmol/l GBP was applied to determine its inhibitory efficacy on various sub-types of HVA calcium channel current.

As shown in Fig. 6, the proportion of N-type Ca^{2+} currents in axotomized neurons was significantly higher (50.0±2.7%) than that in control neurons (35.9±1.4%) and adjacent neurons (37.1±2.0%; P<0.05; Fig. 6B). The contribution of L-type channels to the HVA-Ca^{2+} influx in axotomized neurons was markedly reduced, as 15.4±2.3% of the HVA-Ca^{2+} current was blocked by 20 μmol/l nifedipine compared to 27.9±2.5% in control neurons and 26.1±1.8% in adjacent neurons (P<0.05). There was no significant difference in the proportion of each sub-type of HVA-Ca^{2+} channel current between adjacent and control neurons (P>0.05; Fig. 6B). However, the P/Q-type current was similar between the three groups.

The proportion of N-type Ca^{2+} currents in axotomized neurons was significantly higher (81.0±2.8%) than that in control and adjacent neurons (68.8±4.5 and 69.7±3.3%, respectively; P<0.05), suggesting that the N-type Ca^{2+} channel

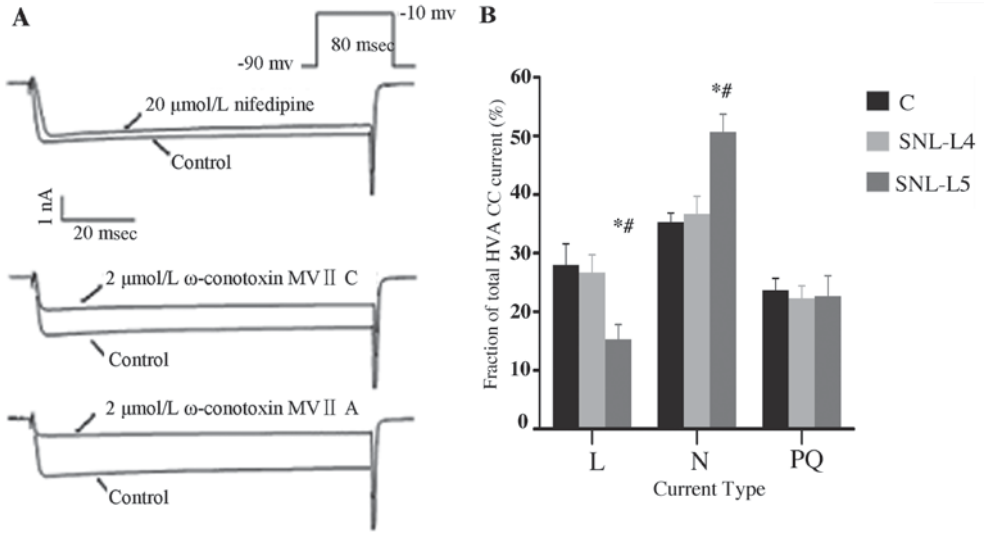

Figure 6. Sub-types of HVA-Ca^{2+} currents identified by application of specific channel blockers. (A) To individually assess various types of calcium channels present in the same cell, 20 μmol/l nifedipine (L-type Ca^{2+}-specific channel blocker), 2 μmol/l ω-conotoxin MVIIC (P/Q-type Ca^{2+} channel-specific blocker) and 2 μmol/l ω-conotoxin MVIIA (N-type Ca^{2+} channel-specific blocker) were applied to the bath in sequence when stable currents were reached. (B) Fraction changes of each sub-type (L, N, P/Q) Ca^{2+} channel current over the total HVA-Ca^{2+} peak currents in control, adjacent and axotomized neurons. Values are expressed as the mean ± standard deviation (n=10). *P<0.05 vs. control neurons (ANOVA); #P<0.05 regarding axotomized vs. adjacent neurons (ANOVA). HVA, high-voltage activation; ANOVA, analysis of variance; SNL, spinal nerve ligation; L4, adjacent neurons; L5, axotomized neurons.

Table II. Sensitive Ca^{2+} current ratios (%) of each channel sub-type (L, P/Q and N) among the three groups.

	HVA-Ca^{2+} subtype		
Group	L	P/Q	N
C	35.2±4.3	43.4±3.5	68.8±4.5
SNL-L4	34.9±3.7	43.6±4.7	69.7±3.3
SNL-L5	32.5±3.4	45.6±4.6	81.0±2.8[a,b]

Values are expressed as the mean ± standard deviation (n=10). [a]P<0.05, compared with the same Ca^{2+} current sub-type of the C group; [b]P<0.05, compared with the same Ca^{2+} current sub-type of the SNL-L_4 group. SNL, spinal nerve ligation; L4, adjacent neurons; L5, axotomized neurons; C, control.

current is the GBP-sensitive sub-type of HVA-Ca^{2+} channel currents (Table II). However, the N- and P/Q-type currents were not affected by GBP.

Discussion

The present study demonstrated that SNL of the peripheral nerve of rats as a model of neuropathic pain injury significantly reduced HVA-Ca^{2+} currents. A decrease in current density, changes in the proportion of HVA-Ca^{2+} channel current sub-types and a depolarizing shift in the voltage dependence of activation appeared to cause this reduction in HVA-Ca^{2+} currents.

According to the I-V curves, the peak current density of axotomized neurons decreased and was lower than that of control and adjacent uninjured DRG neurons. Similar results have been observed in other rat models, including that of chronic constriction injury (CCI). In this model, the somata of acutely dissociated DRG neurons from hyperalgesic rats exhibited a decreased ICa and injury of medium and large neurons decreased the peak calcium channel current density (15). McCallum *et al* (15) examined the ICa specifically in axotomized neurons generated by SNL and indicated that current loss is present in all neuronal size groups. Furthermore, current loss was evident in the adjacent L_4 neurons. These results indicated that various types of nerve injury, such as axotomy, result in ICa loss in primary sensory neurons of all sizes and includes HVA and LVA current types. This may be a common feature of nerve injury (16).

One possible explanation for the reduction in Ca^{2+} currents in DRG neurons observed in the present study is that the calcium channel density in the membrane decreases following axotomy. This may occur due to alterations in channel synthesis or degradation, post-translational modifications affecting the insertion of the channel into the membrane or the transport rate of channels to more distal locations. Alternatively, changes in the single-channel properties of somatic calcium channels may occur (17). The present study compared changes in the HVA-Ca^{2+} channel kinetics in control, adjacent and axotomized DRG neurons in model rats subjected to SNL. It was demonstrated that neuropathic injury shifted the voltage dependence of activation in a depolarized direction, whereas $Vi_{1/2}$ remained unchanged in axotomized and adjacent uninjured DRG neurons. This shift in activation reduced the 'window current' between inactivation and activation, thereby attenuating the sustained inward ICa. A similar decrease in the overlap of the Ca^{2+} influx has previously been observed in a rat model of CCI (18).

The importance of ICa in the functioning of neurons means that altered ICa may contribute to functional abnormalities that accompany neuropathic pain (16). It is possible that the elevated excitability observed in neurons following

axonal injury is the result of diminished ICa. It has been demonstrated that the tetradotoxin-resistant (TTX-R) sodium current provides the greatest amount of total inward current during the downstroke and HVA calcium channels carry a substantial inward current in the form of an AP (19). These currents decreased in the TTX-R sodium channel and HVA calcium channels following axonal injury. The direct effect of ICa contributes to AP formation and admits Ca^{2+} through voltage-dependent calcium channels (VGCCs), which acts on Ca^{2+}-sensitive K^+ channels thus generating inward Ca^{2+} flux through Ca^{2+}-sensitive K^+ channels [IK(Ca)]. In surgery, they contribute to the repolarization of the AP and the generation of AHP (16). AHP determines spike frequency adaptation and the ability of sensory neurons to maintain rapidly firing pulse trains, thus regulating a critical aspect of neuronal excitability (20). There is a correlation between reduced inward ICa and delayed AP depolarization, whereas the outward current, presumably IK(Ca), is reduced at the onset of AHP and during the repolarization phase of the AP (16). Increased burst firing from decreased AHP results in greater nociceptive traffic on the secondary neurons of the dorsal horn, where prolonged AP duration results in greater excitatory neurotransmitter release (16). Increased repetitive firing during sustained depolarization occurs in traumatized nociceptive neurons following axotomy. Thus, axotomized neurons, particularly pain-conducting ones, become unstable and exhibit increased excitability (16).

In the present study, the reduction of peak current density and 'window currents' was observed in adjacent neurons, similar to that in axotomized neurons, due to the injury-induced change of channel activation. L_4 afferent fibers commingled with degenerating L_5 axons in the peripheral nerve, therefore, Wallerian degeneration may result in enhanced excitability of intact neurons with somata in L_4 DRGs adjacent to the axotomized L_5 DRGs. For example, glial cell line-derived neurotrophic factor or nerve growth factor; cytokines, including tumor necrosis factor, interleukin-1 or other inflammatory mediators released by immune cells; and Schwann cells activated by L_5 axonal degeneration, may activate adjacent neurons and lead to hyperexcitability in adjacent neurons, which may result in changes occurring in the distribution and activation state of ion channels (6). Furthermore, intense bursts of activity along the L_5 pathway sensitize the spinal dorsal horn to input along intact (i.e. SNL L_4) pathways, so that natural stimuli are perceived as more intense (16). The process of cross-excitation spreads activity among adjacent neurons in the DRG. The injured adjacent afferents remaining intact following SNL serve a critical role in the development of neuropathic pain by interacting with degenerating afferents and by peripherally-propagating injury discharge, thus inducing peripheral sensitization (21).

The present study revealed that in injured neurons, the proportion of L-type calcium currents decreased and N-type calcium currents increased, whereas the proportion of P/Q-type calcium currents remained unchanged compared with currents in control and adjacent uninjured neurons. Yang *et al* (22) and Sun *et al* (23) observed an upregulation of the N-type Ca^{2+} current in injured DRG neurons in partial sciatic nerve ligation and SNL models, respectively. Hogan *et al* (24) indicated that injury affected the HVA-Ca^{2+} currents of the N- and P/Q-type channels, whereas no effects on the L-type channel current were noted. Another study demonstrated that L-type calcium channel-associated gene expression decreased in rat DRGs following CCI and sciatic nerve axotomy (25). The proportion of N-type calcium currents in adjacent uninjured neurons remained unchanged, which may be due to the inflammatory environment caused by peripheral nerve injury. It has been determined that N-type calcium channel function changes in the rat dorsal horn during inflammation (26). Selective downregulation in the contribution of this calcium channel to excitatory synaptic transmission recorded from neurokinin 1 receptor-positive neurons was observed in the laminae I (26).

Results from animal experiments (27,28) and clinical applications (29) suggest that GBP exhibits significant efficacy in treating chronic pains, particularly neuropathological pain; however, distinct neuroplasticities in various neuropathies may underlie the complexity of the antiallodynic actions of GBP. This indicates that the different effects in treating neuropathological pain may be due to the specific mechanism of nerve injury. The results of the present study demonstrated the dose-dependent inhibition of GBP towards the HVA-Ca^{2+} currents of control, adjacent and axotomized DRG neurons. Following application of 10, 100 and 300 μmol/l GBP, peak current densities decreased in control, adjacent and axotomized neurons, among which the inhibitory effects on the neuronal HVA-Ca^{2+} current of axotomized DRG neurons were more significant. Sarantopoulos *et al* (30) demonstrated that GBP rapidly and reversibly decreased the neuronal peak ICa of sham and neuropathic rats in a concentration-dependent manner; however, with a lack of significant differences in decreases among various groups.

The $Va_{1/2}$ and $Vi_{1/2}$, which were fitted using the Boltzmann equation, indicated a shift towards the hyperpolarized direction, and the 'window current' between the activation curve and the homeostatic inactivation curve changed. An *in vivo* experiment performed by Sutton *et al* (31) revealed that the inhibitory effect of GBP was dose- and voltage-dependent, producing a hyperpolarizing shift in current-voltage curves and reducing the non-inactivating component of the whole-cell current activated at relatively depolarized potentials.

Spinal nerve injury may increase the expression of the VGCC alpha-2-delta-1 sub-unit in the spinal dorsal horn and sensory neurons in the DRG that correlate with established neuropathic pain states (8,32) and GBP-sensitive allodynia (27). The auxiliary $\alpha2\delta$ sub-unit is a membrane-anchored protein and interacts with the extracellular domains of the $\alpha1$ sub-unit. Each auxiliary sub-unit is involved in the trafficking of the channel complex to the membrane and modifies current properties, including the kinetics of activation and inactivation. $\alpha2\delta$ sub-units modify inward calcium currents by regulating the $\alpha1$ sub-unit (33). In addition, co-expression of $\alpha2\delta$ with various α and β sub-units results in the acceleration of current activation and inactivation, an increase in current density and dihydropyridine binding sites, and a hyperpolarising shift of the current-voltage curves (9). The a2δ-1 sub-unit represents the target for gabapentin in the alleviation of hyperalgesia in experimental models of neuropathic pain (34).

The findings of the present study revealed that the mechanism of GBP blockage of HVA calcium channel currents

correlates with the injury-induced changes of activation and inactivation kinetics of the HVA-Ca^{2+} channel.

In the SNL model, alterations of neural signaling in injured and uninjured neurons contributed to the development of neuropathic pain following peripheral nerve injury. However, the pathological mechanisms of the two types of neuronal damage with injured or uninjured neurons differ; the former may mainly be affected by the direct damage of SNL, while the latter primarily arises due to the reaction products associated with Wallerian degeneration following the SNL (35). In the present study, it was observed that the 'window current' decreased in control and axotomized neurons, whereas the 'window current' in adjacent neurons was unchanged following the application of GBP, indicating that its inhibitory effects may depend on the particular neuropathological or inflammatory conditions.

Furthermore, in the present study, there was a certain degree of overlap in the inhibitory effects of various Ca^{2+} channel blockers on the action of GBP. The mixed pharmacology of the GBP-sensitive current suggests that inhibition may reflect the direct action of GBP on a number of different sub-types of calcium channel, dominated by the N-type current in this cell-type, similar to results from the study by Sutton *et al* (31).

Among all VACCs, N-type Ca^{2+} channels, which are potential molecular targets, are considered to be the most important ones in mediating neuropathic pain and the GBP-dependent modulation of pre-synaptic N-type channels in DRG neurons may prove an important means of mediating neuronal excitability and neurotransmitter release (31). In the present study, the proportion of N-type Ca^{2+} currents among the GBP-sensitive Ca^{2+} currents was increased in axotomized neurons, resulting in an increase of the main action target channels of GBP, which may be one of the causes of its enhanced inhibitory effect on HVA-Ca^{2+} currents in injured DRG neurons.

In conclusion, the present study demonstrated that the inhibitory effect of GBP on HVA-Ca^{2+} currents was enhanced in the injured DRG neurons of neuropathic rats. This action may be associated with changes in the activation and inactivation kinetics of Ca^{2+} channels, as well as an increase in the proportion of N-type Ca^{2+} currents. The different effects of GBP on HVA-Ca^{2+} currents in axotomized vs. adjacent neurons may depend on the particular neuropathological condition or inflammatory circumstances induced by peripheral nerve injury.

Acknowledgements

The present study was supported by the Scientific Research Fund of China Post doctorates of the Chinese Government (nos. 20080431417 and 200902694).

References

1. Costigan M, Scholz J and Woolf CJ: Neuropathic Pain: A maladaptive response of the nervous system to damage. Annu Rev Neurosci 32: 1-32, 2009.
2. Sommer C: Neuropathic pain: Pathophysiology, assessment and therapy. Schmerz 27: 619-632, 2013 (In German).
3. Laedermann CJ, Pertin M, Suter MR and Decosterd I: Voltage-gated sodium channel expression in mouse DRG after SNI leads to re-evaluation of projections of injured fibers. Mol Pain 10: 19, 2014.
4. Tsantoulas C, Zhu L, Shaifta Y, Grist J, Ward JP, Raouf R, Michael GJ and McMahon SB: Sensory neuron downregulation of the Kv9.1 potassium channel subunit mediates neuropathic pain following nerve injury. J Neurosci 32: 17502-17513, 2012.
5. Sapunar D, Ljubkovic M, Lirk P, McCallum JB and Hogan QH: Distinct membrane effects of spinal nerve ligation on injured and adjacent dorsal root ganglion neurons in rats. Anesthesiology 103: 360-376, 2005.
6. Ma C, Shu Y, Zheng Z, Chen Y, Yao H, Greenquist KW, White FA and LaMotte RH: Similar electrophysiological changes in axotomized and neighboring intact dorsal root ganglion neurons. J Neurophysiol 89: 1588-1602, 2003.
7. Zhu YF, Wu Q and Henry JL: Changes in functional properties of A-type but not C-type sensory neurons in vivo in a rat model of peripheral neuropathy. J Pain Res 5: 175-192, 2012.
8. Felix R, Calderón-Rivera A and Andrade A: Regulation of high-voltage-activated Ca2+ channel function, trafficking, and membrane stability by auxiliary subunits. Wiley Interdiscip Rev Membr Transp Signal 2: 207-220, 2013.
9. Zhou C and Luo ZD: Electrophysiological characterization of spinal neuron sensitization by elevated calcium channel alpha-2-delta-1 subunit protein. Eur J Pain 18: 649-658, 2014.
10. Hooker BA, Tobon G, Baker SJ, Zhu C, Hesterman J, Schmidt K, Rajagovindan R, Chandran P, Joshi SK, Bannon AW, *et al*: Gabapentin-induced pharmacodynamic effects in the spinal nerve ligation model of neuropathic pain. Eur J Pain 18: 223-237, 2014.
11. Kukkar A, Bali A, Singh N and Jaggi AS: Implications and mechanism of action of gabapentin in neuropathic pain. Arch Pharm Res 36: 237-251, 2013.
12. Kim SH and Chung JM: An experimental model for peripheral neuropathy produced by segmental spinal nerve ligation in the rat. Pain 50: 355-363, 1992.
13. Choi Y, Yoon YW, Na HS, Kim SH and Chung JM: Behavioral signs of ongoing pain and cold allodynia in a rat model of neuropathic pain. Pain 59: 369-376, 1994.
14. Harper AA and Lawson SN: Conduction velocity is related to morphological cell type in rat dorsal root ganglion neurons. J Physiol 359: 31-46, 1985.
15. McCallum JB, Kwok WM, Sapunar D, Fuchs A and Hogan QH: Painful peripheral nerve injury decreases calcium current in axotomized sensory neurons. Anesthesiology 105: 160-168, 2006.
16. Hogan QH: Role of decreased sensory neuron membrane calcium currents in the genesis of neuropathic pain. Croat Med J 48: 9-21, 2007.
17. Baccei ML and Kocsis JD: Voltage-gated calcium currents in axotomized adult rat cutaneous afferent neurons. J Neurophysiol 83: 2227-2238, 2000.
18. McCallum JB, Kwok WM, Mynlieff M, Bosnjak ZJ and Hogan QH: Loss of T-type calcium current in sensory neurons of rats with neuropathic pain. Anesthesiology 98: 209-216, 2003.
19. Blair NT and Bean BP: Roles of tetrodotoxin (TTX)-sensitive Na+ current, TTX-resistant Na+ current, and Ca2+ current in the action potentials of nociceptive sensory neurons. J Neurosci 22: 10277-10290, 2002.
20. Lirk P, Poroli M, Rigaud M, Fuchs A, Fillip P, Huang CY, Ljubkovic M, Sapunar D and Hogan Q: Modulators of calcium influx regulate membrane excitability in rat dorsal root ganglion neurons. Anesth Analg 107: 673-685, 2008.
21. Jang JH, Lee BH, Nam TS, Kim JW, Kim DW and Leem JW: Peripheral contributions to the mechanical hyperalgesia following a lumbar 5 spinal nerve lesion in rats. Neuroscience 165: 221-232, 2010.
22. Yang L and Stephens GJ: Effects of neuropathy on high-voltage-activated Ca (2+) current in sensory neurones. Cell Calcium 46: 248-256, 2009.
23. Sun XD, Zhu MM, Chen XD, Li D, Wang Q, Xiao H, Xu JG and Duan ML: Effects of gabapentin on high-voltage-activated calcium current in dorsal root ganglion neurons in rats. Zhonghua Yi Xue Za Zhi 91: 1713-1717, 2011 (In Chinese).
24. Hogan QH, McCallum JB, Sarantopoulos C, Aason M, Mynlieff M, Kwok WM and Bosnjak ZJ: Painful neuropathy decreases membrane calcium current in mammalian primary afferent neurons. Pain 86: 43-53, 2000.
25. Kim DS, Yoon CH, Lee SJ, Park SY, Yoo HJ and Cho HJ: Changes in voltage-gated calcium channel alpha(1) gene expression in rat dorsal root ganglia following peripheral nerve injury. Brain Res Mol Brain Res 96: 151-156, 2001.

26. Rycroft BK, Vikman KS and Christie MJ: Inflammation reduces the contribution of N-type calcium channels to primary afferent synaptic transmission onto NK1 receptor-positive lamina I neurons in the rat dorsal horn. J Physiol 580: 883-894, 2007.
27. Luo ZD, Calcutt NA, Higuera ES, Valder CR, Song YH, Svensson CI and Myers RR: Injury type-specific calcium channel alpha 2 delta-1 subunit up-regulation in rat neuropathic pain models correlates with antiallodynic effects of gabapentin. J Pharmacol Exp Ther 303: 1199-1205, 2002.
28. Gauchan P, Andoh T, Ikeda K, Fujita M, Sasaki A, Kato A and Kuraishi Y: Mechanical allodynia induced by paclitaxel, oxaliplatin and vincristine: Different effectiveness of gabapentin and different expression of voltage-dependent calcium channel alpha(2)delta-1 subunit. Biol Pharm Bull 32: 732-734, 2009.
29. Gabapentin for Adults with Neuropathic Pain: A Review of the Clinical Evidence and Guidelines. Ottawa (ON): Canadian Agency for Drugs and Technologies in Health; 2014.
30. Sarantopoulos C, McCallum B, Kwok WM and Hogan Q: Gabapentin decreases membrane calcium currents in injured as well as in control mammalian primary afferent neurons. Reg Anesth Pain Med 27: 47-57, 2002.
31. Sutton KG, Martin DJ, Pinnock RD, Lee K and Scott RH: Gabapentin inhibits high-threshold calcium channel currents in cultured rat dorsal root ganglion neurones. Br J Pharmacol 135: 257-265, 2002.
32. Boroujerdi A, Zeng J, Sharp K, Kim D, Steward O and Luo ZD: Calcium channel alpha-2-delta-1 protein upregulation in dorsal spinal cord mediates spinal cord injury-induced neuropathic pain states. Pain 152: 649-655, 2011.
33. Benedikt Nimmervoll: The function of the Ca2+ channel α2δ subunits in synaptic release in hippocampal neurons.
34. Lana B, Schlick B, Martin S, Pratt WS, Page KM, Goncalves L, Rahman W, Dickenson AH, Bauer CS and Dolphin AC: Differential upregulation in DRG neurons of an α2δ-1 splice variant with a lower affinity for gabapentin after peripheral sensory nerve injury. Pain 155: 522-533, 2014.
35. Meyer RA and Ringkamp M: A role for uninjured afferents in neuropathic pain. Sheng Li Xue Bao 60: 605-609, 2008.